

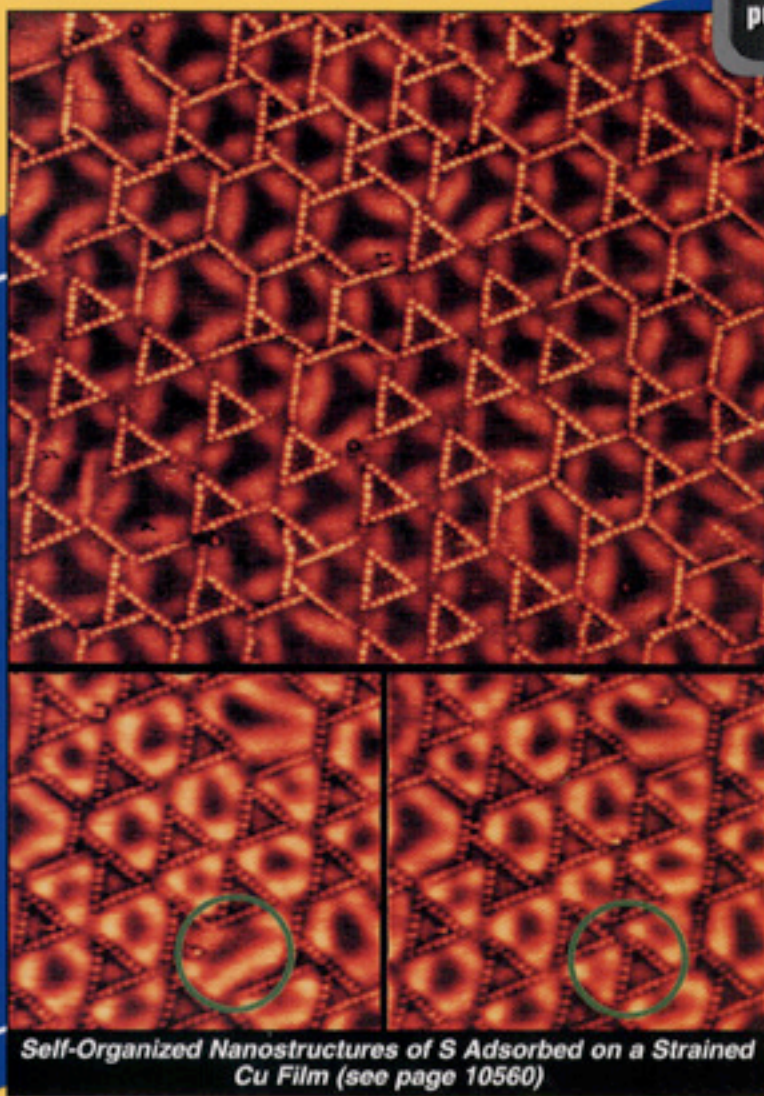
The Journal of Physical Chemistry B

Volume 103

December 2, 1999

Number 48

ON THE WEB
pubs.acs.org/JPCB



*Self-Organized Nanostructures of S Adsorbed on a Strained
Cu Film (see page 10560)*

**CONDENSED MATTER,
MATERIALS, SURFACES,
INTERFACES, & BIOPHYSICAL**



PUBLISHED WEEKLY BY THE AMERICAN CHEMICAL SOCIETY

A Prelude to Surface Chemical Reaction: Imaging the Induction Period of Sulfur Interaction with a Strained Cu Layer

J. Hrbek,^{*,†} J. de la Figuera,[‡] K. Pohl,[‡] T. Jirsak,[†] J. A. Rodriguez,[†] A. K. Schmid,[‡] N. C. Bartelt,[‡] and R. Q. Hwang[‡]

Chemistry Department, Brookhaven National Laboratory, Upton, New York 11973-5000, and
Surface Chemistry Department, Sandia National Laboratories, Livermore, California 94551-0969

Received: July 23, 1999; In Final Form: September 22, 1999

The induction period of the chemical reaction between Cu and S was visualized with STM, revealing a complex interplay between strain relief and reaction mechanism. Copper sulfide formation, monitored by high-resolution soft X-ray photoemission, started only after adsorption of ~ 0.2 ML of S on a two-atom thick Cu layer supported by a Ru(0001) substrate. The pre-sulfide stages of sulfur interaction were investigated by in situ STM. Sulfur decorated the Cu surface by adsorbing at pseudo 4-fold hollow sites of the striped Cu phase and restructured the Cu layer to create additional adsorption sites of this type. Several self-organized structures of adsorbed S on the dynamically responding strained Cu layer were observed. Significant structural changes of both adsorbate and adsorbent occurred within the induction period of this surface chemical reaction.

Introduction

Studies of sulfur interaction with metal surfaces are important for understanding the poisoning in catalysis and corrosion in material science. Ultrathin metal films play a significant role in science and technology: their reactivity and stability have a broad impact in diverse technological areas within the chemical and electronic industries. These films are often strained, containing misfit dislocations. Their structure is different from the bulk and consequently their chemical reactivity is altered. As the reaction proceeds, the strain state of the metal film can also change, allowing additional adsorption of reactants. Thus there can be a complex feedback between strain state and chemisorption. Here we address questions related to the very early stages of the interaction of sulfur with Cu, using STM to visualize the behavior of both adsorbed sulfur and the copper layers.

Strain in surfaces is caused by abrupt termination of the bulk, or by lattice mismatch in the case of films deposited on dissimilar substrates. The surface reconstruction of a single-crystal surface may result as a consequence of the former, while dislocations in a film reflect the latter. Typical examples are "herringbone" reconstruction of a Au(111) surface,¹ and layer-dependent dislocation phases of Cu film grown on Ru(0001) surfaces.² A delicate balance between the strain energy needed for surface structural rearrangement and the interface energy required for the formation of a relaxed interface can be easily disrupted by adsorption. The adsorption energy of the adsorbate can shift the energy balance, causing the surface to adopt a different configuration. While there are many cases of adsorbate-induced reconstruction known for clean metal surfaces, less is known about the adsorbate interactions with strained films,³ where one might expect even more dramatic effects because of the larger strains one can create. In this letter we report such a

study for the case of a two-atom-thick copper film supported on a Ru(0001) substrate interacting with sulfur.

Experimental Section

Films were grown by physical vapor deposition of Cu from a calibrated metal doser at pressures below 2×10^{-10} Torr on carefully cleaned Ru(0001). Deposition at $T < 500$ K was followed by flash anneal to 700 K, and the surface was examined by STM at room temperature. Sulfur was generated by a solid-state electrochemical doser and deposited on the surface at 300 K at $p < 5 \times 10^{-10}$ Torr. Sulfur exposure estimates were based on the total pressure measurements, and S coverages were estimated from the STM images. Images are shown in a gray scale representation, with lighter areas representing either higher parts of the surface or higher tunneling current. To monitor the chemical state of the surface, photoemission spectra of samples prepared by an identical procedure were measured at the U7A beamline of the National Synchrotron Light Source. The S 2p spectra reported here were acquired using a photon energy of 260 eV, the binding energy scale was calibrated against the position of the Fermi edge, and coverage calibration was based on the H₂S-saturated Ru (0001) surface.

Results and Discussion

The first Cu layer on Ru(0001) grows pseudomorphically, adopting the structure of the Ru substrate. Because the lattice constant of Cu is 5.5% smaller than that of Ru, the first Cu layer is under tensile strain. A sequence of strain-relieved structures develops for thicker copper film: the second and third layers have distinct networks of misfit dislocations and the fourth layer has an in-plane lattice constant close to bulk Cu.^{2,4}

An anisotropically relaxed second Cu layer, consisting of 3 domains of double stripes with a periodicity of ~ 4.3 nm running along $\langle 1\bar{2}1 \rangle$ directions is shown in Figure 1A. The bright stripes are misfit dislocations buried at the Cu–Ru interface separating regions of fcc and hcp stacking (Figure 1B). The Cu atoms in a near bridge position with respect to the Ru substrate are higher

* Author to whom correspondence should be addressed. E-mail: hrbek@bnl.gov.

[†] Brookhaven National Laboratory.

[‡] Sandia National Laboratories.

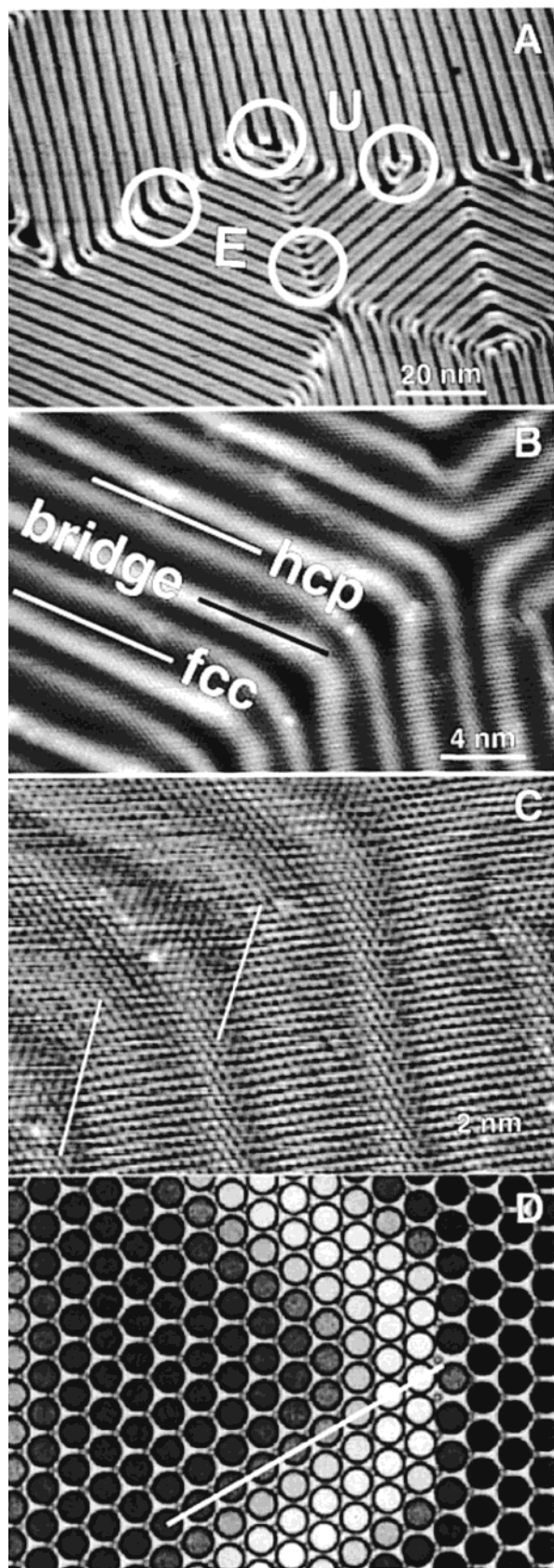


Figure 1. Three domains of Cu second layer striped phase adsorbed on Ru(0001): (A) Large scale image with the dislocation edges at the domain wall labeled E (elbows) and U (U-turns); (B) higher-resolution image showing the alternating arrangement of Cu adatoms at different adsorption sites; (C) high-resolution image of the edge dislocations with rows of extra Cu adatoms indicated by lines; (D) Frenkel-Kontorova model of the edge dislocation showing details of surface structure: extra Cu rows and pseudo 4-fold adsorption sites.

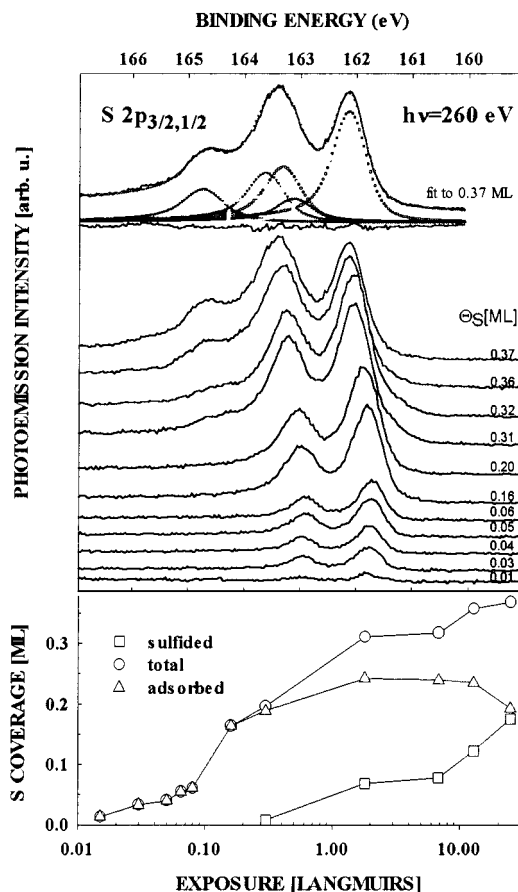


Figure 2. S 2p core level spectra for S adsorption on striped Cu layer supported on a Ru(0001) surface. The spectra were fitted with up to three S 2p doublets (upper panel) and the integrated intensity of the individual contributions is displayed in the lower panel. Sulfur coverage calibration is based on the S 2p data from a Ru(0001) surface saturated by H₂S at room temperature.

and appear brighter in the image. Across the dislocations, i.e., along the $\langle 110 \rangle$ directions, the strain is almost fully relaxed. Along the lines in the $\langle 1\bar{2}1 \rangle$ directions the Cu atoms are still under considerable tensile stress.

Elbows (labeled E in Figure 1A), or short and long U-turns (labeled U) are the meeting points of misfit dislocations. Geometry dictates⁵ that at these points a dislocation of pure edge character must thread out of the film. The extra row of Cu atoms terminates at the core of the emerging threading edge dislocation and the ideal 3-fold hollow adsorption sites are distorted into pseudo 4-fold hollow sites. Atomically resolved images show the distortion of the adsorption sites at the edge dislocation (Figure 1C), and Frenkel-Kontorova model calculations agree with the experimentally observed structure (Figure 1D).⁶

Figure 2 shows S 2p spectra after exposure of the ~ 2 ML thick Cu layer to sulfur. The first spectra in the set display a well-defined S 2p_{3/2,1/2} doublet with the 2p_{3/2} component at a binding energy of 161.85 eV, an energy characteristic of adsorbed atomic sulfur.^{7,8} The inset shows the sulfur uptake curve based on the curve fitted and integrated experimental data. Increase in the integrated peak intensity with no concurrent change in the peak position is seen through spectra up to $\Theta_s = 0.06$ ML. Although the photoemission data suggest efficient sticking of sulfur they also point to the exclusive presence of adsorbed atomic sulfur in the early stage of the Cu-S interaction.

After the initial adsorption of ~ 0.20 ML a weak shoulder

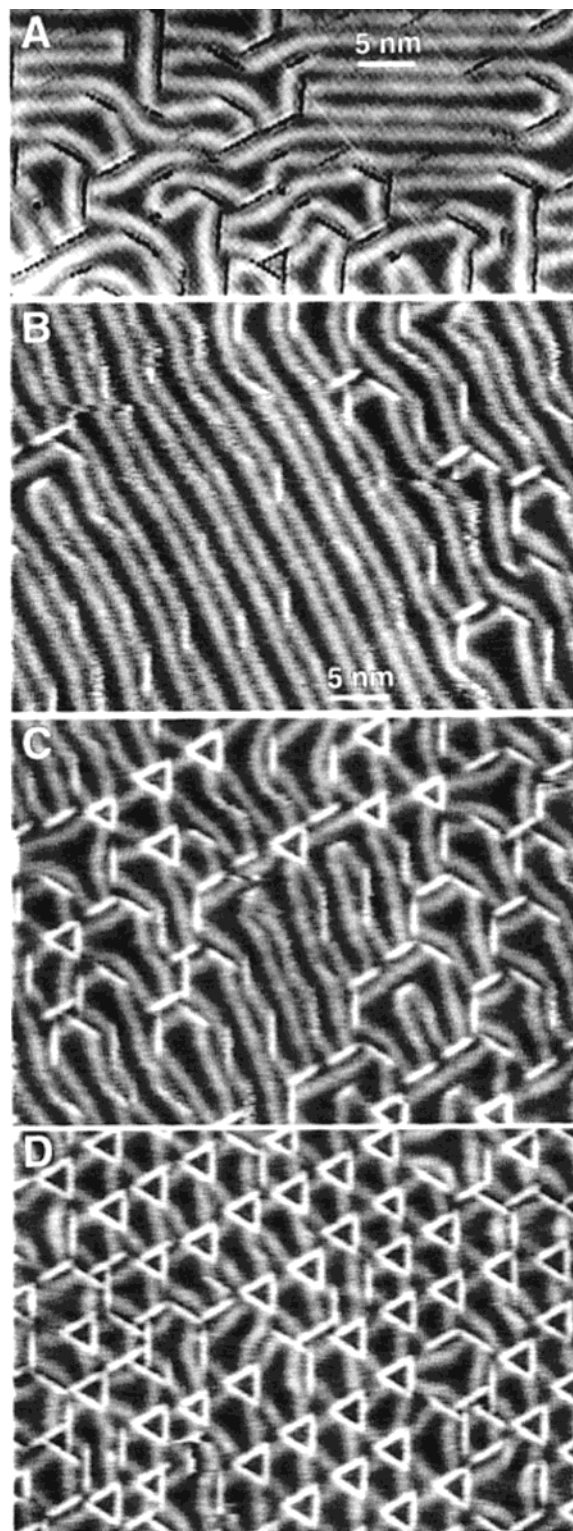


Figure 3. (A) Early stages of S adsorption on the striped Cu layer. Individual S adatoms imaged as black dots are arranged in short rows and are found at the edge dislocations and less frequently on stripes. Estimated S coverage < 0.01 ML; (B–D) Development of sulfur features with increasing S coverage: sulfur adatoms self-organize in rows, hexagons, and equilateral triangles. Sulfur rows can be imaged either as dark or bright lines depending on the tip status (see McIntyre, B. J.; Sautet, P.; Dunphy, J. C.; Salmeron, M.; Somorjai, G. A. *J. Vac. Sci. Technol. B* **1994**, *12*, 1751).

appears on the high binding energy side of photoemission curve. This shoulder intensifies with sulfur exposure and at $\Theta_S = 0.37$ ML a new peak at 164.5 eV is well defined while the leading peak has shifted by 0.5 eV to higher binding energy. The

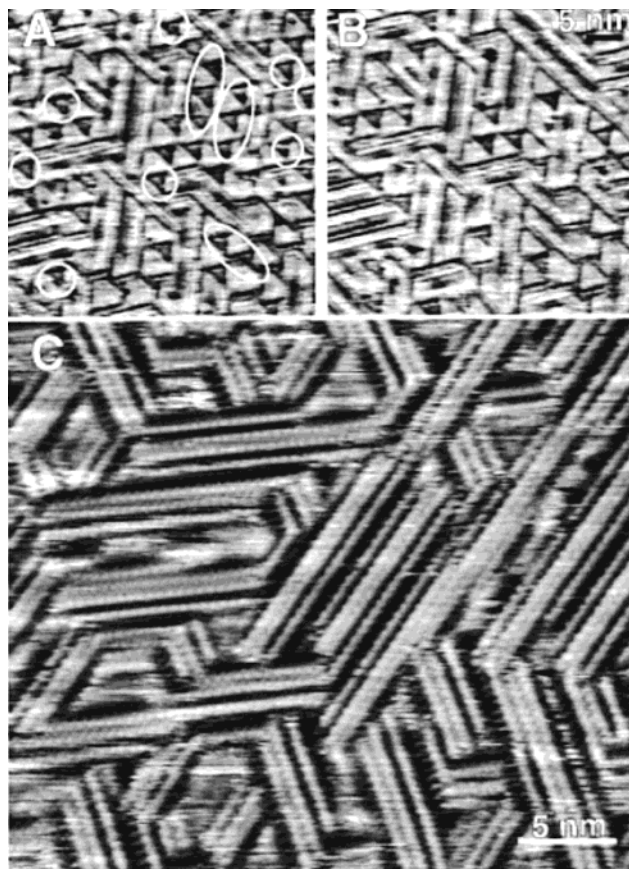


Figure 4. Final stages of structural changes of striped Cu layer. As Θ_S increases the close-packed array of triangles converts into the ribbon phase: (A) and (B) Two time-lapsed images taken 720 s apart acquired during S deposition. The disappearing triangles are highlighted; (C) higher-resolution image of the ribbon structure.

complex envelopes of the spectra were curve fitted⁹ with up to three S $2p_{3/2,1/2}$ doublets as shown for the 0.37 ML curve in the upper part of Figure 2. Two higher-energy doublets are assigned to sulfide S 2p core levels in agreement with data from bulk samples.⁷ The shift of the low-energy doublet associated with atomic S is caused by adsorption of S in the vicinity of copper sulfide. The intensity of the sulfide peaks grows with increasing S dose, while that of the adsorbed S levels off and even decreases.

The long induction period is unusual for reactive elements such as S and Cu. To determine the cause we used STM to visualize structural changes of the surface. We image the S adatoms as sharp protrusions (Figure 3A). At very low S coverages ($\Theta_S \sim 0.001$ ML) sulfur adsorbs mainly at the edge dislocations. From the atomically resolved STM images we see that sulfur adatoms are arranged in straight lines with 4 or 8 atoms, depending on the type of the edge dislocation.¹⁰

We argue that S adatoms are first trapped at pseudo 4-fold sites. Such sites, found on the clean striped Cu surface, are aligned along $\langle 110 \rangle$ at the edge dislocations with a nearest-neighbor (NN) distance of ~ 0.26 nm. The measured S–S distance of ~ 0.55 nm suggests that the S adatoms occupy the next-nearest-neighbor sites. The formation of small $p(2 \times 2)$ -S islands on Ru(0001) at room temperature and low S coverages¹¹ implies the NN repulsive interactions between S adatoms, and similar interactions may exist for the one-dimensional S lines. The sulfur interaction with the striped Cu phase substrate reflects the nonuniformity of the strained surface. The only energetically competitive adsorption sites on the striped Cu layer are therefore

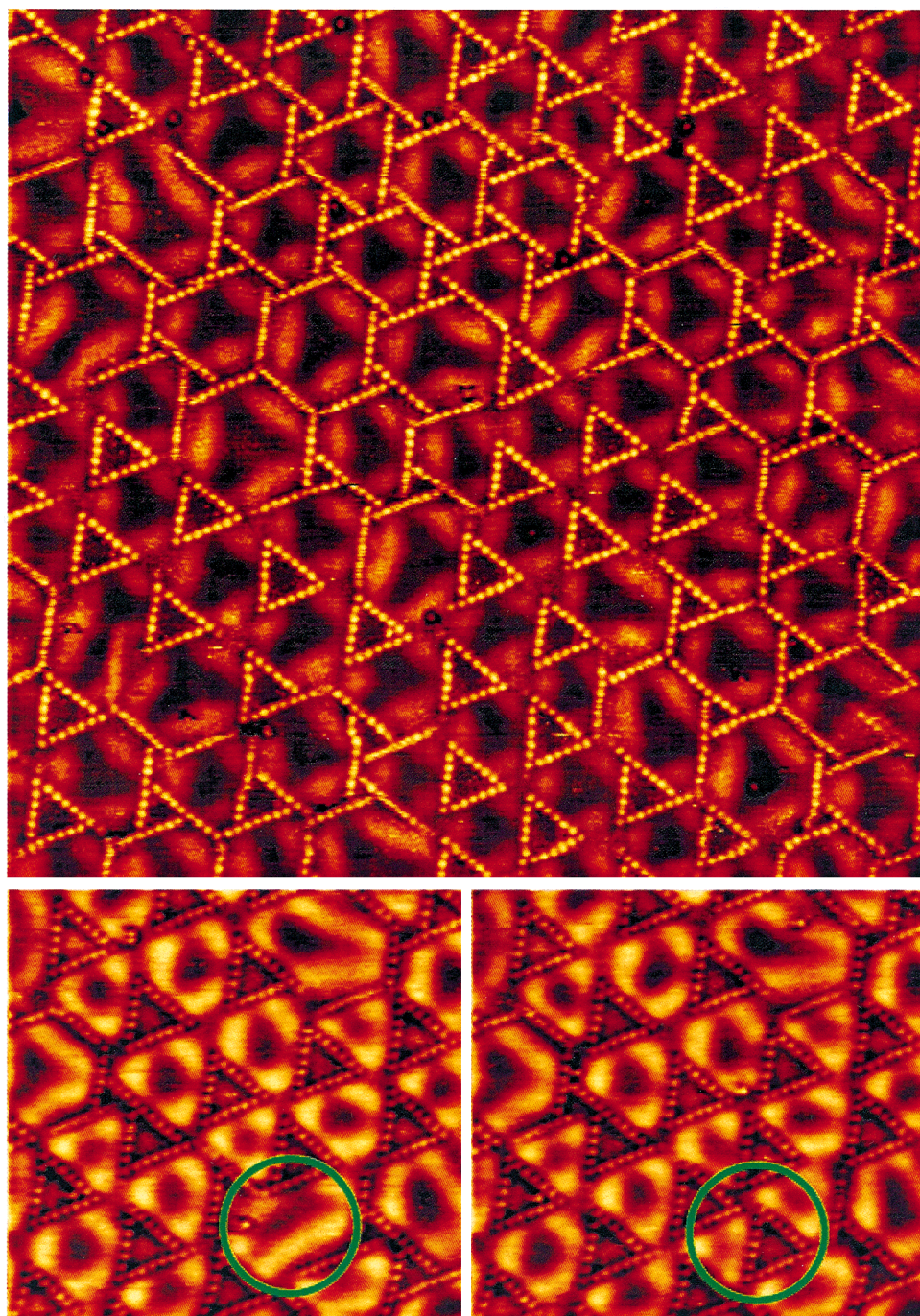


Figure 5. An image (7.3 nm \times 6.9 nm) of S self-organized in hexagons and equilateral triangles made of 18 sulfur adatoms. At room temperature and fixed S/Cu stoichiometry ($\Theta_S \sim 0.03$ ML for this image) the observed structural patterns fluctuate for hours. Lower two time-lapse images (3.5 nm \times 3.3 nm) taken 50 s apart show formation of new equilateral triangles.

the 4-fold coordinated ones, while the 3-fold coordinated sites have potentials that are too shallow to trap S adatoms at room temperature. The net result is formation of the short straight lines of adsorbed S atoms where the NN repulsion leads to adsorption at every second adsorption site on the Cu substrate.

An alternative explanation of the observed structure is that the lines of S are molecular sulfur. At first sight this might seem reasonable. Solid elemental sulfur has a strong tendency to catenation: a large number of allotropic forms are known, the most stable of which is cyclooctasulfur. However, both the S–S distance of 0.205 nm and the S–S–S angle of 106° in the S allotropes¹² are very different from our measurements, thus excluding any possibility of the existence of molecular sulfur on the striped Cu surface. Further support of our model comes

from the fact that the drive to occupy high coordination sites is strong in the case of sulfur as shown by a S-driven pseudo- $\{100\}$ reconstruction of Ni and Cu $\{111\}$ surfaces.^{13,14}

Images in Figure 3 show that additional edge dislocations are formed by both dissociation of the existing edge dislocations and nucleation of new ones as sulfur coverage increases.¹¹ (Interestingly, at fixed S/Cu stoichiometry, images display thermal fluctuations of the dislocation network on a time scale of minutes over a period of several hours.)

The Cu surface thus accommodates more sulfur atoms as Θ_S increases (Figure 3B–D). The misfit dislocations are cut in regular intervals by S adatoms that adsorb again in straight lines with the same S–S distance of 0.55 nm. The rows have 4 to 8 S atoms and run parallel to $\langle \bar{1}10 \rangle$ directions. A plausible scenario

for the formation of short segments of misfit dislocations is an elastic response of the mostly uniaxially strained Cu layer. Copper atoms in the strips along $\langle\bar{1}2\bar{1}\rangle$ are under tensile stress that can be presumably relieved in the presence of adsorbed S at the edge dislocations by a slip of the misfit dislocation along the $\langle\bar{1}10\rangle$ direction. Such a slip creates pseudo 4-fold sites that are promptly filled with S.

There are similarities between sulfur and oxygen interacting with the striped Cu layer in these early stages. Adsorption of oxygen also starts at the edge dislocations and is followed by cuts of the misfit dislocations. However, the individual O adatoms were not resolved.¹⁵

As the S coverage increases further, the short segments of misfit dislocations bend and form trigons, the fcc regions bounded by a dislocation loop made up of three edge dislocations that are connected by three curved misfit dislocations. Simultaneously sulfur rows self-organize into a network of hexagons and close-packed equilateral S-triangles made of 18 atoms that bound the hcp stacking areas (Figure 5, top). This self-organizing network of sulfur hexagons evolves toward a more stable network of S triangles and compact misfit dislocation loops (Figure 5, bottom). Sulfur thus removes the uniaxial strain observed in the second layer along the $\langle\bar{1}2\bar{1}\rangle$ direction and isolates the areas of hcp and fcc stacking.

The formation of this dense trignon network of misfit dislocations implies that the density of Cu atoms in the bilayer is increasing with increasing S coverage. (The higher the Cu density, the larger the number of misfit dislocations needed to accommodate the increased strain.) Similar trignon dislocation networks are found on the dense third layer of clean Cu/Ru(0001).^{2,4,16} In the case of the clean Cu, the increased density is due to the fact that three layers of Cu are more like bulk than the bilayer.¹⁶ In our case there are two possible explanations for the increased density. The first one is that S lowers the energy cost of making the misfit dislocations, allowing more Cu atoms into the bilayer. The second possibility is that adsorbed S on Cu might increase the tensile strain of the film—i.e., prefer shorter Cu—Cu bonds—thus increasing the driving force for the formation of misfit dislocations. We cannot distinguish these two mechanisms on the basis of our data. Nevertheless it is clear that there is a complex interplay between chemical reactivity and the introduction of these misfit dislocations.

With sulfur coverage above 0.05 ML a new S structure appeared. The network of triangles is converted into ~ 3 nm wide ribbons of parallel S-rows aligned along $\langle\bar{1}2\bar{1}\rangle$ directions (Figure 4). The conversion starts at defect sites (such as distorted trigons) of the close-packed array of equilateral triangles. The triangles disintegrate and sulfur is realigned in straight long rows, with three rows bundled together to form the ribbon (Figure 4C). The uniform width of ribbons corresponds to the height of the triangles while the length varies from 4 to 30 nm reflecting the number of triangles that fell apart to create the ribbon. The image quality at these higher S coverages is, however, degraded and the details of conversion cannot be ascertained experimentally. Only at this moment we see the first indication of sulfide formation as the shoulder on the higher-binding-energy side of the main S 2p doublet (Figure 2).

Summary

The limited reactivity of the striped Cu layer seems to be caused by the small number of reactive adsorption sites preexisting on the surface. As sulfur adsorbs at these active sites, identified as the pseudo 4-fold sites in this work, additional active sites are created by a dynamic rearrangement of the Cu

surface. The Cu surface goes through several restructuring phases, each of them visualized by characteristic sulfur patterns. This sequential restructuring underpins the induction period and is necessary before the actual chemical conversion of metallic Cu to Cu sulfide begins.

There are several broader implications of these results. First, sulfur can be used as an effective probe of adsorption sites and surface interactions and is comparable to CO that was used as a probe molecule to study the structural, morphological, and electronic properties of Cu layers on Ru(0001).¹⁷ Direct visualization of both substrate and adsorbate provides a unique insight into previously unknown phases in surface interactions. Second, STM studies of surface chemical reactions may provide long-sought experimental data supporting Taylor's concept of active sites¹⁸ and their role in catalysis and relation to structure-sensitive reactions. Thirty years ago Thomas¹⁹ suggested that dislocations might be active sites for surface chemical reactions. Recent experimental²⁰ and theoretical²¹ work, together with the results of this work, have proved this hypothesis. Third, heterogeneous metal catalysts are usually small metal clusters supported on metal oxide substrates.²² Such metal clusters may be significantly strained and we can therefore expect their surface chemical reactivity to be different from that of the fully relaxed surface of a bulk metal. In relating structure, dynamics, and reactivity of adsorbates on surface the STM and the AFM are starting to play a substantial role.^{23–26}

Acknowledgment. This research was carried out at Brookhaven and Sandia National Laboratories and was supported by the U.S. Department of Energy, Office of Basic Energy Sciences under Contract Nos. DE-AC2-98CH10886 and DE-AC04-94AL8500. JdIF is thankful for financial support from the Spanish MEC (PB 96-02710).

References and Notes

- (1) Wöhl, C.; Chiang, S.; Wilson, R. J.; Lippel, P. H. *Phys. Rev. B* **1989**, *39*, 7988.
- (2) Pötschke, G. O.; Behm, R. J. *Phys. Rev. B* **1991**, *44*, 1442.
- (3) Titmuss, S.; Wander, A.; King, D. A. *Chem. Rev.* **1996**, *96*, 1291.
- (4) Günther, C.; Vrijmoeth, J.; Hwang, R. Q.; Behm, R. J. *Phys. Rev. Lett.* **1995**, *74*, 754.
- (5) Carter, C. B.; Hwang, R. Q. *Phys. Rev. B* **1995**, *51*, 4730.
- (6) Bartelt, N. C.; de la Figuera, J.; Hamilton, J. C. In preparation.
- (7) Kuhn, M.; Rodriguez, J. A. *J. Phys. Chem.* **1994**, *98*, 12059.
- (8) Hrbek, J.; Li, S. Y.; Rodriguez, J. A.; van Campen, D. G.; Huang, H. H.; Xu, G.-Q. *Chem. Phys. Lett.* **1997**, *267*, 65.
- (9) Hrbek, J.; van Campen, D. G.; Malik, I. J. *J. Vac. Sci. Technol. A* **1995**, *13*, 1409.
- (10) de la Figuera, J.; Pohl, K.; Schmid, A. K.; Bartelt, N. C.; Hrbek, J.; Hwang, R. Q. *Surf. Sci.* **1999**, *433–435*, 93.
- (11) Hrbek, J.; Schmid, A. K.; Bartelt, N. C.; Hwang, R. Q. *Surf. Sci.* **1997**, *385*, L1002.
- (12) Meyer, M. *Chem. Rev.* **1976**, *76*, 367.
- (13) Woodruff, D. P. *J. Phys.: Condens. Matter* **1994**, *6*, 6067.
- (14) Foss, M.; Feidenhans, R.; Nielsen, M.; Findeisen, E.; Buslaps, T.; Johnson, R. L.; Besenbacher, F. *Surf. Sci.* **1997**, *388*, 15.
- (15) de la Figuera, J.; Pohl, K.; Schmid, A. K.; Bartelt, N. C.; Hwang, R. Q. *Surf. Sci.* **1998**, *415*, L993.
- (16) Hamilton, J. C.; Foiles, S. M. *Phys. Rev. Lett.* **1995**, *75*, 882.
- (17) Hoffmann, F. M.; Paul, J. *J. Chem. Phys.* **1987**, *86*, 2990; *ibid.* **1987**, *87*, 1857.
- (18) Taylor, H. S. *Adv. Catal.* **1948**, *1*, 1.
- (19) Thomas, J. M. *Adv. Catal.* **1969**, *19*, 293.
- (20) Gsell, M.; Jakob, P.; Menzel, D. *Science* **1998**, *280*, 717.
- (21) Mavrikakis, M.; Hammer, B.; Nørskov, J. K. *Phys. Rev. Lett.* **1998**, *81*, 2819.
- (22) Ertl, G.; Freund, H. J. *Phys. Today* **1999**, *52*, 32.
- (23) Winterlin, J.; Volkening, S.; Janssens, T. V. W.; Zambelli, T.; Ertl, G. *Science* **1997**, *278*, 1931.
- (24) Stipe, B. C.; Rezaei, M. A.; Ho, W. *Science* **1998**, *280*, 1732.
- (25) Pohl, K.; Bartelt, N. C.; de la Figuera, J.; Bartelt, N. C.; Hrbek, J.; Hwang, R. Q. *Nature* **1999**, *397*, 238.
- (26) Giancarlo, L. C.; Flynn, G. W. *Annu. Rev. Phys. Chem.* **1998**, *49*, 297.